Felling, Tim

Working Paper

Solving the bi-level problem of a closed optimization of electricity price zone configurations using a genetic algorithm

HEMF Working Paper, No. 09/2019

Provided in Cooperation with:
University of Duisburg-Essen, Chair for Management Science and Energy Economics

Suggested Citation: Felling, Tim (2019) : Solving the bi-level problem of a closed optimization of electricity price zone configurations using a genetic algorithm, HEMF Working Paper, No. 09/2019, University of Duisburg-Essen, House of Energy Markets & Finance, Essen

This Version is available at:
https://hdl.handle.net/10419/201592

Solving the Bi-level Problem of a Closed Optimization of Electricity Price Zone Configurations using a Genetic Algorithm

HEMF Working Paper No. 09/2019

by

Tim Felling

July 2019

UNIVERSITÄT DUISBURG ESSEN

Open-Minded

Solving the Bi-level Problem of a Closed Optimization of Price Zone Configurations in Europe using a Genetic Algorithm by Tim Felling

Abstract

The topic of alternative price zone configurations is frequently discussed in Central Western Europe where – so far – national borders coincide with borders of price zones. Reconfiguring these price zones is one option in order to improve congestion management, foster trading across borders of price zones and, thus, to increase welfare. In view of the significant increase in redispatch volumes and costs over the last years due to increasing feed-in from renewable energy sources in conjunction with delayed grid expansion, this topic has gained in importance. To determine these improved price zone configurations for a large-scale system like Central Western Europe, often either configurations based on expert guesses are considered or heuristics using approximate criteria like locational marginal prices are used to obtain price zones through clustering. In contrast, the present paper formulates a bi-level optimization problem of how to determine optimal configurations in terms of system costs and – given the size and nature of the problem – solves it with a specially developed genetic algorithm. Resulting price zone configurations are compared to both exogenously given, expert-based price zone configurations from the Entso-E bidding zone study and endogenously assessed configurations from a hierarchical cluster algorithm. Results show that the genetic algorithm achieves best results in terms of system costs. Moreover, the comparison with solutions from a hierarchical cluster analysis reveals important drawbacks of the latter methodology.

Keywords: price zone configuration, bidding zone configuration, cluster algorithm, genetic algorithm, evolutionary algorithm, locational marginal prices

JEL-Classification: C38, C61, D47, L5, Q48

Tim Felling
House of Energy Markets and Finance
University of Duisburg-Essen, Germany
Universitätsstr. 12, 45117 Essen

+49-(0)201 / 183-6706
Tim.felling@uni-due.de
www.hemf.net

Content

Abbreviations

CBCO	Critical branches Critical Outages
CWE	Central Western Europe
CWE+	Extended Central Western Europe
DA	Day-ahead
Fref	Reference flow
GA	Genetic algorithm
GSK	Generation Shift Key
HCA	Hierarchical cluster algorithm
MC(C)	Market clearing (costs)
NTC	Net transfer capacities
PTDF	Power transfer distribution factor
PZ(C)	Price zone (configuration)
RD(C)	Redispatch (costs)
RAM	Remaining available margin
SC	System costs

Nomenclature

$A_{f,i}$	Nodale PTDF
$A_{f,z}$	Zonale PTDF
b€	Billion €
C^{comp}	Costs for redispatch (RD), day-ahead (DA) or system (SC)
$c_{g,h}$	Variable costs of generator g in hour h
$d_{i,h}$	Demand at node i in hour h
$f \in F^{CBCO}$	Line f of the set of CBCOs F
$g_{g,h}^{RD+/-}$	Positive (+) or negative (-) redispatch from generator g in hour h
$g_{g,h}^{DA}$	Infeed of generator g in hour h on day-ahead market
$g_{g,h}^{max/min}$	Maximum/minimum generation of generator g in hour h

G_z^{max}	Maximum capacity of generators in zone z
$g \in G$	Generator g of set of generators G
$h \in H$	Hour h of the set of considered hours H
κ_i	Generation shift key at node i
k€	Thousand €
L_f^{FRM}	Flow reliability margin on line f
L_f	Thermal capacity of line f
$L_{f,h}^{DA}$	Capacity of line f in hour h on the DA market (RAM)
$M_{z,i}^{N2Z}$	Assignment Matrix of nodes to zones
$M_{g,i}^{G2N}$	Assignment Matrix of generators to nodes
m€	Million €
n_Z	Fixed number of zones
$\phi_{f,h}^{BC}$	Flow on line F in hour h in the base case
$\phi_{f,h}^{DA}$	Reference Flow (Fref) of line f in hour h
$q_{z,h}$	Zonal net position of zone z in hour h
γ	Mark-up factor for redispatch costs
Z	Set of zones z

1 Introduction

Electricity markets in Europe are constantly evolving. One driver is the call for further integration, notably with the introduction of the so-called Flow-Based market coupling (FBMC) approach for the day-ahead (DA) market in 2015. This new form of zonal market coupling superseded the previously net transfer capacity- (NTC) based market coupling aiming at a better representation of the physics of the underlying electricity grid and an increase of welfare. However, when evaluating welfare of European electricity markets, a comprehensive assessment has to go beyond the consideration of the DA market and has to comprise redispatch costs as well. Targeted climate goals and increasing capacities of flexible, variable renewables put the electricity grid under increasing stress. In conjunction with delayed grid expansion this results in increasing redispatch (RD) amounts and costs (including also curtailment of renewables), namely around 1.2 billion euros in Germany in 2017 compared to 200 million euros in 2014 (c.f. (Bundesnetzagentur, 2019; Bundesverband der Energie- und Wasserwirtschaft e.V. (BDEW), 2018)). Thus, the role of congestion management becomes more important and questions the current market design in Europe with zonally coupled price zones (PZs).

A frequently discussed solution approach in both academia and politics is the reconfiguration of price zones to align PZ borders to frequently congested lines instead of national borders. An overview over contributions is presented in sec. 2. Entso-E has even launched an official review of the current existing zones and investigates potential reconfigured PZs. Yet, no quantitative results of market or redispatch models have been presented in the study (ENTSO-E, 2018).

Given the significance of this topic, the paper at hand presents a methodology to identify improved price zone configurations (PZCs) for Central Western Europe (CWE). It formulates a bi-level optimization problem that aims at finding the optimal PZCs with least system costs. On the lower level, the costs of DA market under a FBMC regime and on the upper level the costs for redispatch are minimized. The computation is challenging, as the problem is applied on the entire grid of CWE. Moreover, the inclusion of the PZC as a decision variable leads to a highly non-linear problem. To this end, a genetic algorithm is developed to solve the problem. This comprises the development of individual genetic operators that are explicitly tailored for the particular optimization problem. Given the nature of genetic algorithms, the identified solutions are most likely not optimal, but at least improved PZCs. The resulting PZCs are evaluated for their system costs in contrast to other configurations. On the one hand, they are compared to PZCs from a hierarchical cluster algorithm (HCA) which is based on nodal prices (LMPs) (cf. (Felling and Weber, 2018)) and on the other hand to expert-based PZCs from the Bidding Zone Study (ENTSO-E, 2018). A nodal pricing set-up serves as another benchmark. Moreover, the performance of the algorithm and its genetic operators is investigated.

The paper at hand is organized as follows. In sec. 2, extant literature is presented and the novelty and contribution of the paper at hand is underlined. Thereafter, in sec. 3, the problem formulation of the optimization problem is presented. Subsequently, sec. 4 introduces the corresponding solution approach, namely the developed GA. Sec. 5 explains the evaluation methodology. Finally, results are presented in sec. 6 while sec. 7 gives a summary and concludes the paper at hand.

2 Literature Review

In energy economics literature, nodal pricing is frequently considered as the optimal market design. Several publications point out its advantages such as (Bjørndal and Jörnsten, 2001, 2007; Ehrenmann and Smeers, 2005; Hogan, 1992; Schweppe et al., 1988). However, a zonal pricing regime, where borders of price zones usually align with national borders, is still present in CWE and a development directly to nodal pricing, as implemented in parts of the US or New Zealand (Consentec and Neon, 2018; Biggar, Darryl R.; Hesamzadeh, 2014), is unlikely to materialize soon. A more likely approach constitutes the determination of alternative, improved PZCs.

There are numerous publications that investigate improved PZCs. Relevant existing literature of how to identify and evaluate alternative PZCs can be clustered into three streams:

- The first one relates to exogenously given configurations. In both (Trepper et al., 2015) and (Egerer et al., 2016) the authors split Germany into two PZs, a Northern and Southern zone. Both studies show that RD amounts can be reduced while price spreads between the two zones, except for a few hours, remain relatively small. In these works, as the split is given exogenously, focus lays on the assessment and evaluation of these exogenous alternative PZCs.
- The second stream looks at different approaches to assess PZCs endogenously by the use of heuristics, i.e. various cluster algorithms. These heuristics are based on different easily computable yet approximate criteria. Most algorithms cluster locational marginal prices (LMPs) or power transfer distribution factors (PTDFs). LMPs are clustered by (Burstedde, 2012) who uses a hierarchical algorithm based on Ward's criterion on a simplified grid of CWE. (Breuer, 2014) uses a genetic algorithm to cluster LMPs of the European transmission system into PZs[1]. In (Felling and Weber, 2018), the authors apply a hierarchical algorithm using demand- and infeed-weighted nodes to investigate a robust configuration for different economic scenarios for CWE. The same algorithm is then applied in (Felling et al., 2019) where improved PZCs are compared in a large-scale

[1] Parts of the dissertation (Breuer, 2014) are published in (Breuer and Moser, 2014; Breuer et al., 2013). Henceforth it is referred to (Breuer, 2014) as the main reference.

model system. Therein, the authors show that a reconfiguration of PZs can reduce system costs significantly, especially due to decreasing redispatch costs (RDC). Further algorithms based on LMPs are applied in (Wawrzyniak et al., 2013; Imran and Bialek, 2008). In contrast to the LMP-based methodology, cluster algorithms based on PTDFs are applied by (Bergh et al., 2016; Sarfati et al., 2015; Klos et al., 2014; Kang et al., 2013; Wawrzyniak et al., 2013; Duthaler et al., 2012). (Bergh et al., 2016) also investigate improved PZCs for CWE and Italy, Czech Republic and Poland. The investigations consider the impact of the improved PZCs on zonal network parameters, line flows and fuel shares.

- The third stream also refers to endogenously assessed PZCs. In contrast to the second stream, authors set up optimization problems to identify optimal PZCs rather than using heuristics based on approximate criteria. (Grimm et al., 2017) formulate a three-level problem that includes the configuration of PZs on the first level while on the second and third level the DA market and RD measures are optimized. In (Bjørndal and Jörnsten, 2001) authors also formulate an optimization problem. However, as stated in their paper, the problem is hard to solve due to the "non-linear and discrete nature of the problem" (Bjørndal and Jørnsten 2001, p. 71). Moreover, the application on a large-scale system of such optimizations problems with thousands of nodes is computationally too challenging (Felling and Weber, 2018; Breuer, 2014). Thus, (Grimm et al., 2017) investigate networks with only up to 28 nodes. The proposed optimization problem in (Bjørndal and Jörnsten, 2001) remains unsolved.

The paper at hand combines all three streams while focusing on the combination of stream three and two. In line with stream three, the paper presents a bi-level optimization problem of how to identify an optimal PZC with the explicit objective function of minimizing overall system costs. The DA market and the RD stage are considered on separate levels. However, as improved PZCs for the entire extended CWE (CWE+)[2] with over 2200 nodes are desired and the inclusion of a PZC as a decision variable leads to a highly non-linear problem (cf. sec. 3), a heuristic methodology is required to solve this bi-level problem. In line with stream two, a genetic algorithm (GA) is developed and applied to the CWE+ electricity grid. The algorithm takes the GA of (Breuer, 2014) as a starting point, but differs in its methodology in two respects. On the one hand, it directly considers system cost minimization in the objective function (instead of the approximate criterion of LMP variation). On the other hand, a new genetic operator is developed and existing ones are adapted and tailored to the specific optimization problem. Finally, in line with stream one, the PZCs are evaluated against other PZCs. Results are compared to exogenously

[2] CWE+ comprises Germany, France, Belgium, the Netherlands, Austria and Switzerland

given PZCs such as the current PZC in CWE+ but also to the suggested PZCs from the ENTSO-E Bidding Zone Study (BZS) (ENTSO-E, 2018). Moreover, in order to prove the effectiveness of the developed algorithm, results are compared to PZCs from the LMP-based hierarchical cluster algorithm of (Felling and Weber, 2018). The market outcome of a nodal pricing set-up serves as a benchmark for all PZCs, as it is often referred to as the theoretically economic optimum (as mentioned in the beginning of this section).

Having said that, one important feature of the algorithm is the consideration of FBMC procedures for the DA market coupling. The principles of FBMC and the determination of its parameters have been outlined in previous publications. A summary of the main features is given in sec. 3 and, for now, we refer to the works of (Felten et al., 2019; Marjanovic et al., 2018; Wyrwoll et al., 2018; Van den Bergh et al., 2016; Marien et al., 2013) for detailed information.

In terms of GAs, developments go back to the works of (Holland, 1975) and (Goldberg and Holland, 1989). The general advantage of these kinds of algorithms is the applicability to large-scale problems and that their genetic operators are suitable for different kinds of problems. Their solution is likely to be a local optimum instead of the global optimum in most cases. Thus, often a trade-off between computation times and optimality has to be considered (Tovey, 2018). An overview over GAs is given in, among others, (Mitchell, 1998; Srinivas and Patnaik, 1994).

In conclusion, the paper at hand is the first that combines all three above-mentioned streams: The advantages of a mathematical foundation and objective function that explicitly targets the minimization of system costs, the application and development of a heuristic solver, namely a GA, and the comparison to other endogenous and exogenous configurations.

3 Problem Formulation

This section presents the problem formulation of the developed bi-level problem of identifying an optimal PZC.

3.1 Problem Structure

Figure 1 presents a general overview of the problem structure. In chronological order and as presented in (Grimm et al., 2017), the problem can be formulated as a three-level problem as visualized on the left-hand side in Figure 1. At first, a regulator decides on a PZC. Subsequently, the DA market is carried out. In case of network congestions, RD actions are undertaken by the system operator.

Subsequently, the problem size is reduced to form a bi-level problem. To this end, we take advantage of the fact that the regulator and the system operator share the same objective function of minimizing overall system costs. This enables a combination of the third and first level to a

new first level, a so-called "system perspective". A similar approach is also used in (Grimm et al., 2017). The newly restructured two-level problem is presented on the right-hand side of Figure 1.

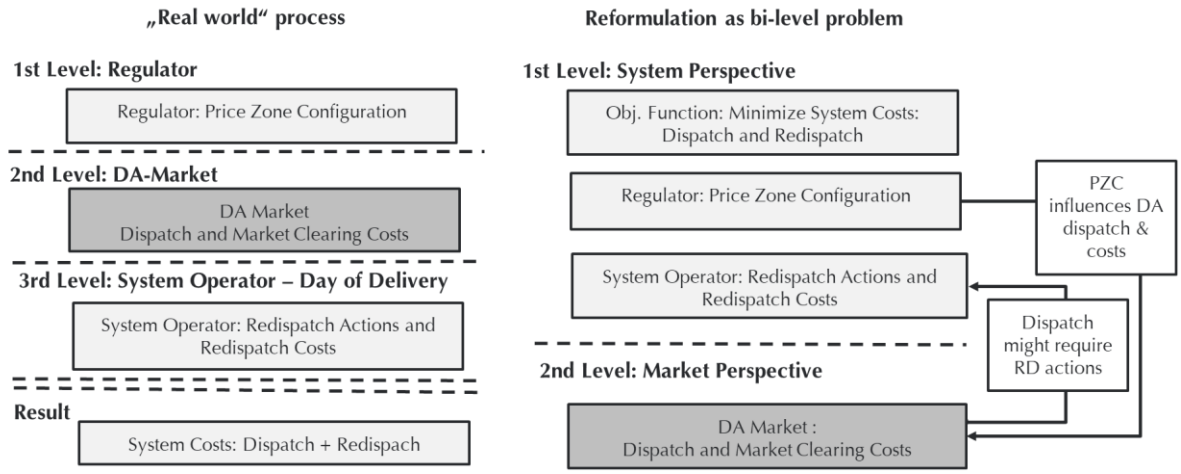

Figure 1: Structure of optimization problem

The minimization of system costs (SC), i.e. minimizing the sum of market clearing costs (MCC) and redispatch costs (RDC), constitutes the upper level objective. Given a PZC on the upper level, the FBMC optimization problem on the lower level is solved for this given PZC. Its results, mainly costs and power plant dispatch, are handed back to the upper level. Therein, the determined dispatch is tested for potential violation of network constraints and, thus, whether RD measures are necessary.

3.2 Upper Level Problem

The upper level of the introduced bi-level problem is described in this section, while the following section focusses on the corresponding lower level. Eq. (1) presents the upper level objective function namely the minimization of SC, i.e. the sum of both MCC $C_{g,h}^{DA}$ and RDC $C_{g,h}^{RD}$ per generator is minimized over all considered hours. Notably, no inter-temporal constraints are considered. Thus, the bi-level problem can be computed for each hour separately. This is of importance for the algorithm introduced later, since it enables a parallelization of the computation. The PZC enters the optimization problem in form of the binary matrix $M_{z,i}^{N2Z}$ that is among the optimization variables. The particular role of the matrix is introduced at the end of this section.

$$\min_{M_{z,i}^{N2Z}, g_{g,h}^{RD+}, g_{g,h}^{RD-}, g_{g,h}^{DA}} C^{SC}$$

with

$$C^{SC} = C^{DA} + C^{RD} = \sum_{h} \sum_{g} C_{g,h}^{DA} + C_{g,h}^{RD} \qquad (1)$$

The overall RDC C^{RD} are determined as presented in eq. (2). The variables $g_{g,h}^{RD+}$ and $g_{g,h}^{RD-}$ denote positive and negative redispatch quantities of a generator g in the hour h. The set H denotes the set of considered hours. The output is constrained by the remaining flexibility, i.e. the delta between the maximum $g_{g,h}^{max}$ and minimum capacity $g_{g,h}^{min}$ and the DA-generation $g_{g,h}^{DA}$. The **generation constraints** are given in eq. (3) and (4).[3] Notably, the DA-generation is determined in the lower level problem.

$$C^{RD} = \sum_h (\sum_g (c_{g,h}((1+\gamma) g_{g,h}^{RD+} - (1-\gamma) g_{g,h}^{RD-})) \quad (2)$$

$$g_{g,h}^{DA} - g_{g,h}^{RD-} \geq g_{g,h}^{min} \; \forall \; g \in G, h \in H \quad (3)$$

$$g_{g,h}^{RD+} + g_{g,h}^{DA} \leq g_{g,h}^{max} \; \forall g \in G, \; h \in H \quad (4)$$

The factor γ entering the RDC and thus the objective function (cf. eq. (1)) serves as a mark-up factor to penalize RD actions. In this paper, γ is set to 0.2 to account for inefficiencies in the RD process and to prevent a re-optimization of the DA market outcome. The RD modelling approach is based on (Felling et al., 2019). Therein, the same factor is applied and authors also present a sensitivity for different γ- values. Setting $\gamma = 0$ would correspond to fully efficient RD. In that case, as (Voswinkel et al., 2019) explain in a similar context, the solution from the DA market (i.e. the lower level problem) would not matter, as the DA solution would be backshifted by RD to the optimal nodal solution without additional costs (RDC could even be negative). In case of perfectly efficient RD, the sum of RDC and MCC is the same for any given PZCs and equals the SC of the nodal solution. That is due to the optimality of the nodal solution. It yields the cost-minimal dispatch that does not violate any constraints (cf. (Voswinkel et al., 2019)).

The following constraints complete the upper-level equations and correspond to those of a nodal pricing set-up. For the RD assessment, the complete electricity grid is considered, i.e. all nodes i, lines f, and the complete **nodal PTDF** $A_{f,i}$. Net injections are considered on a nodal level by the variable $q_{i,h}$. It consists of the generation according to the DA market solution $g_{g,h}^{DA}$ and potential curative positive $g_{g,h}^{RD+}$ or negative $g_{g,h}^{RD-}$ generation from RD measures, subtracted by the corresponding load (demand) value $d_{i,h}$ (eq. 7). The assignment matrix $M_{g,i}^{G2N}$ (generator-to-nodes) is used to distribute infeed from generators to nodes. The **transmission constraint** is given by eq. (5). L_f denotes the thermal capacity of a line f.[4] Eq. (6) presents the **balance constraint**.

[3] In this paper, the minimum capacity of generator is set to zero. Yet, in an advanced application the parameter could differ from zero, e.g. in order to reflect must-run constraints.
[4] The capacity is reduced to 85% to approximate n-1 security.

$$-L_f \leq \sum_i A_{f,i} q_{i,h} \leq L_f \; \forall \; f \in F, h \in H \tag{5}$$

$$\sum_i q_{i,h} = 0 \; \forall \; h \in H \tag{6}$$

$$q_{i,h} = \left(\sum_g \left(g_{g,h}^{DA} + g_{g,h}^{RD+} - g_{g,h}^{RD-}\right) M_{g,i}^{G2N}\right) - d_{i,h} \; \forall \; i \in I, h \in H \tag{7}$$

Finally, the aforementioned binary **node-to-zone (N2Z) matrix $M_{z,i}^{N2Z}$** constitutes the remaining optimization variable from eq. (1). In view of the focus on PZCs of this paper, the matrix is of particular importance. A PZC may be broken down to an assignment of nodes to zones. This assignment is translated into the binary matrix $M_{z,i}^{N2Z}$. Every node is assigned to one and only one PZ. This is ensured by eq. *(8)*. Each zone consists of at least one node (cf. eq. *(9)*).

$$\sum_z M_{z,i}^{N2Z} = 1 \; \forall \; i \in I; \tag{8}$$

$$\sum_i M_{z,i}^{N2Z} \geq 1 \; \forall \; z \in Z; \tag{9}$$

Furthermore, a set of constraints ensures connectivity of zones meaning that all nodes in a zone have to be connected. This can be formulated via a graph-theoretical approach as shown in (Grimm et al., 2017). In the present paper, the Matlab® graph toolbox is used during the application of the algorithm.

Finally, the number of price zones is fixed from the outset (cf. eq. (10)). Without that fix, the node-to-zone matrix $M_{z,i}^{N2Z}$ would converge to the optimal solution of a nodal set-up with each node being a zone. As aforementioned, the nodal solution is the solution with the lowest costs that satisfies all constraints. Due to the mark-up factor γ, any RD actions cause additional costs. Hence, the optimizer would try to reduce RD by downsizing zones until either each node is a single zone or at least very small zones are identified that do not cause RD in any considered time step.

$$card(Z) = n_Z \tag{10}$$

As eq.(*1*) to (*7*) suggest, the PZC $M_{z,i}^{N2Z}$ does yet not directly affect the upper level problem. Given the nodal set-up of the redispatch assessment, the complete grid with every node is considered and, thus, is not directly affected by any PZCs. That is different for the lower level problem, as the following section shows.

3.3 Lower Level Problem

The lower level problem replicates FBMC procedures for the DA market clearing. Given the objective of this paper to identify improved PZCs, the focus in the following descriptions lies not only on FBMC but also on how the PZC is considered in the optimization problem. Moreover, in reference to (Voswinkel et al., 2019), the differences between the upper (nodal) and lower (zonal)

level are worked out. As previously indicated, only the DA problem is directly influenced by the PZCs and, thus, by the matrix $M_{z,i}^{N2Z}$.

The objective function aims at minimizing MCC on the DA market and formulates as follows:

$$\min_{g_g^{DA}} C^{DA}$$

with

$$C^{DA} = \sum_h \sum_g c_{g,h} g_{g,h}^{DA} \tag{11}$$

The corresponding constraints replicate current FBMC procedures. As several publications present how FBMC parameters can be derived and explain their basic functionalities, only the key aspects are summarized here (c.f. (Felten et al., 2019; Voswinkel et al., 2019; Marjanovic et al., 2018; Wyrwoll et al., 2018; Van den Bergh et al., 2016; Amprion et al., 2014; Marien et al., 2013)). Two days before delivery, FBMC parameters are generated by linearizing the electricity grid around a base-case, the best estimation for the day of delivery (Schavemaker et al., 2008).[5] These parameters comprise **zonal PTDFs** that correspond to a weighted nodal PTDF (cf. eq. *(12)*). In contrast to the upper level, nodes are not considered individually but via the aggregated zonal PTDF. The PZC in terms of $M_{z,i}^{N2Z}$ is thereby of importance as it determines the assignment of nodes to zones.

$$A_{f,z} = \sum_i A_{f,i} \cdot \kappa_i \cdot M_{z,i}^{N2Z} \; \forall \, f \in F, z \in Z \tag{12}$$

The applied weights κ_i are called **generation shift keys (GSKs).** They express how a change of the zonal net position $q_{z,h}$ is shifted on the nodes of a zone. In the paper at hand, so-called capacity weighted GSKs are chosen (cf. eq. *(13)*).[6] For these GSKs, the PZC is required in two ways. First, to determine the entire generation capacity of a zone G_z^{max} (cf. eq. *(14)*). Second, to serve as an assignment operator of G_z^{max} in the denominator of eq. *(13)*.

$$\kappa_i = \frac{\sum_g \left(M_{g,i}^{G2N} \cdot g_g^{max} \right)}{\sum_z G_z^{max} \cdot M_{z,i}^{N2Z}} \; \forall \, i \in I \tag{13}$$

$$G_z^{max} = \sum_i \sum_g M_{z,i}^{N2Z} \cdot \left(M_{g,i}^{G2N} \cdot g_g^{max} \right) \forall \, z \in Z \tag{14}$$

For the zonal balance $q_{z,h}$ the information on the nodal level $q_{i,h}^{DA}$ (cf. eq.*(15)*) is grouped to a zonal level $q_{z,h}$ (cf. eq. *(16)*).

[5] In the present paper, the nodal solution is considered for the base-case assumption. (Wyrwoll et al., 2018) apply a two-stage model to generate a (zonal) base-case. (Finck et al., 2018) use an NTC approach.
[6] To derive GSKs, various methodologies exist (cf. (Voswinkel et al., 2019; Dierstein, 2017; Van den Bergh et al., 2016))

$$q_{i,h}^{DA} = (\sum_g g_{g,h}^{DA} \cdot M_{g,i}^{G2N}) - d_{i,h} \; \forall \; i \in I, \; h \in H \qquad (15)$$

$$q_{z,h} = \sum_i M_{z,i}^{N2Z} \cdot q_{i,h}^{DA} \; \forall \; z \in Z, h \in H \qquad (16)$$

The other important set of parameters are the **remaining available margins** $L_{f,h}^{DA}$ (**RAMs**, cf. eq. (*17*)). They reflect the available line capacity given by its thermal capacity and reduced by a security margin (so-called flow reliability margin (FRM), L_f^{FRM})[7] and a reference flow ($\phi_{f,h}^{DA}$). This flow represents the delta between the expected flow from the base case ($\phi_{f,h}^{BC}$, cf. eq. (*19*)) with expected nodal net positions $q_{i,h}^{BC}$ and the flow that results from the zonal approximation (zonal PTDF) at the same generation and demand pattern (Felten et al., 2019; Amprion et al., 2014). The reference flow results from substituting eq. (*19*) into eq. *(18)*.

$$L_{f,h}^{DA} = L_f - L_f^{FRM} - \phi_{f,h}^{DA} \; \forall \; f \in F^{CBCO}, \; h \in H \qquad (17)$$

$$\phi_{f,h}^{DA} = \phi_{f,h}^{BC} - \sum_z A_{f,z} \cdot q_{z,h}^{BC} \; \forall \; f \in F^{CBCO}, \; h \in H \qquad (18)$$

$$\phi_{f,h}^{BC} = \sum_z A_{f,i} \cdot q_{i,h}^{BC} \; \forall \; f \in F^{CBCO}, \; h \in H \qquad (19)$$

While at the upper level all lines are considered with their physical capacity (cf. eq. (*5*) in the problem set-up), line constraints at the lower level differ in two ways. Again, the PZC is of importance:

First, not all lines but only a set of critical branches and outages (CBCO) F^{CBCO} is considered in the FBMC problem formulation. This set, depending on the parametrization of FBMC, consists of all cross-border lines and eventually some internal, so-called critical branches.[8] Thus, when changing the PZCs, the considered cross-border lines and accordingly the set F^{CBCO} changes as well. Second, as shown in eq. (*17*), the line capacity is reduced by the reference flow ($\phi_{f,h}^{DA}$) and a security margin (L_f^{FRM}). The reference flow is impacted by the zonal PTDF and, thus, the PZC as well.

Having introduced the FBMC parameters and the role of the PZC in terms of $M_{z,i}^{N2Z}$, the **transmission constraint** is presented in eq.*(20)*. The line flow, i.e. the product of zonal PTDF and zonal net positions, has to be within the transmission capacities. Accordingly, eq. *(21)* and eq. *(22)* present the **balance constraint** and the **generation constraint**.[9]

[7] In the paper at hand, we set the FRM L_f^{FRM} to zero. (e.g. as applied in (Bjørndal and Bjørndal, 2017))

[8] In the paper at hand, we only consider cross-border lines (e.g. as also applied in (Bjørndal and Bjørndal, 2017)). It is currently under discussion, whether internal branches are to be considered in future FBMC (cf. (ACER, 2018)) as they shall not hamper trade between price zones.

[9] Again, as in the upper level, $g_g^{min}$is set to zero for the application in this paper.

$$-L_{f,h}^{DA} \leq \sum_z A_{f,z} q_{z,h} \leq L_{f,h}^{DA} \ \forall \ f \ \in F^{CBCO},\ h \in H \qquad (20)$$

$$\sum_z q_{z,h} = 0, \forall\ h \in H \qquad (21)$$

$$g_g^{min} \leq \ g_g^{DA} \leq g_g^{max} \forall\ g \ \in G \qquad (22)$$

In general, constraints at the upper-level (RD) and lower level (DA) are related. The main difference lies in the granularity of the considered system. In the RD problem, a nodal set-up, including all lines, nodes and their corresponding net positions, is considered. In the DA-problem, only the zonal net exports and the sub-set of critical branches are considered (see above-mentioned (Voswinkel et al., 2019) for a comparison of nodal and zonal system). The PZC, respectively the node-to-zone assignment matrix $M_{z,i}^{N2Z}$, affects the lower level in several ways. It is used to aggregate nodes to zones for the zonal PTDFs (i), for the GSKs (ii), the assessment of zonal net-position (iii), the assessment of reference flows (iv) and the set of considered branches (v).

The above listing and corresponding equations highlight that the lower-level problem is (highly) non-linear in the matrix $M_{z,i}^{N2Z}$ (cf. eq. *(12)* to *(14)*, *(16)* to *(18)*, *(20)*and *(21)*). Apart from that, both problems are linear in the other variables. The non-linearity, in conjunction with the problem size, is one of the main reasons for using the GA that is introduced in the following section.

4 Solution Approach: Genetic Algorithm

While section 3 has presented the formulation of the optimization problem, this section introduces the developed solution algorithm. As stated in the introduction, GAs are suitable for large-scale applications and nonlinear, mixed integer optimization problems.

The general idea of GAs is to create a so-called population of candidate solutions. These candidates are then iteratively adjusted by different genetic operators. Exemplary classic operators are the crossover operator, where parts of two or more candidate solutions are merged, or the mutation operator which adjusts single parts of a candidate solution. A mixture of operators has to ensure both diversification (or exploration) and intensification (exploitation) of results (c.f. (Tovey, 2018; Mitchell, 1998; Holland, 1975)). After each iteration, the candidate solutions with the best objective value (also called fitness value) in conjunction with the best solutions from the population database are taken to the next iteration. The following subsection explains the developed algorithm and presents its developed genetic operators.

4.1 General overview

Figure 2 visualizes the flowchart of the algorithm and its elements. Starting with the initial population (start solution) and its evaluation, all steps of the algorithm are presented in the following subsections.

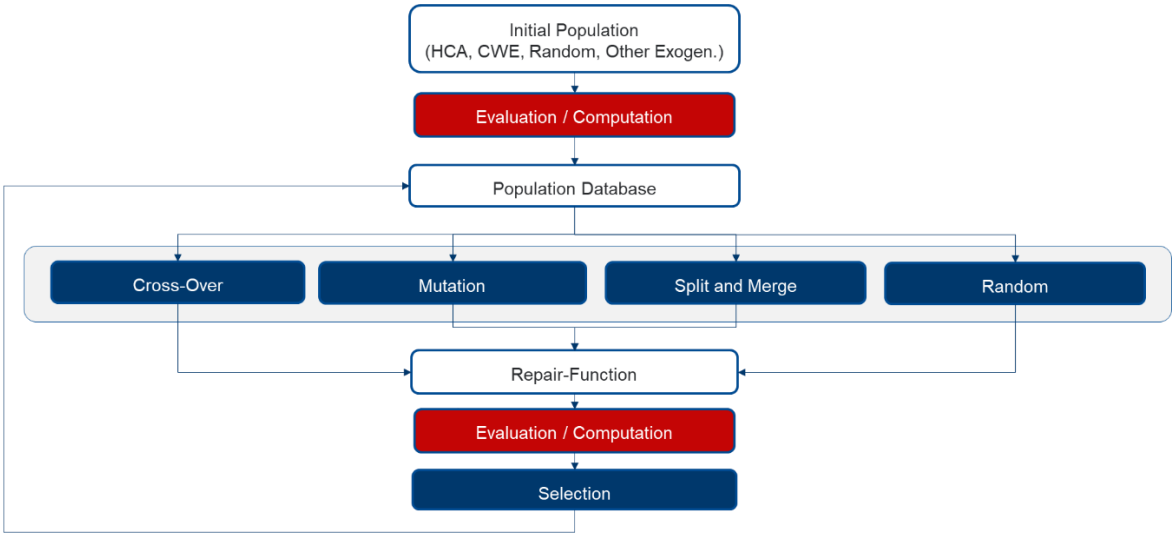

Figure 2: Flowchart of genetic algorithm

4.2 Initial Population

Starting point of the algorithm is an initial population i.e. a set of candidate solutions. Each candidate solution corresponds to a PZC whereby the binary matrix $M_{z,i}^{N2Z}$ is rewritten as an assignment vector as visualized in Figure 3. A similar approach has been applied in (Breuer, 2014).

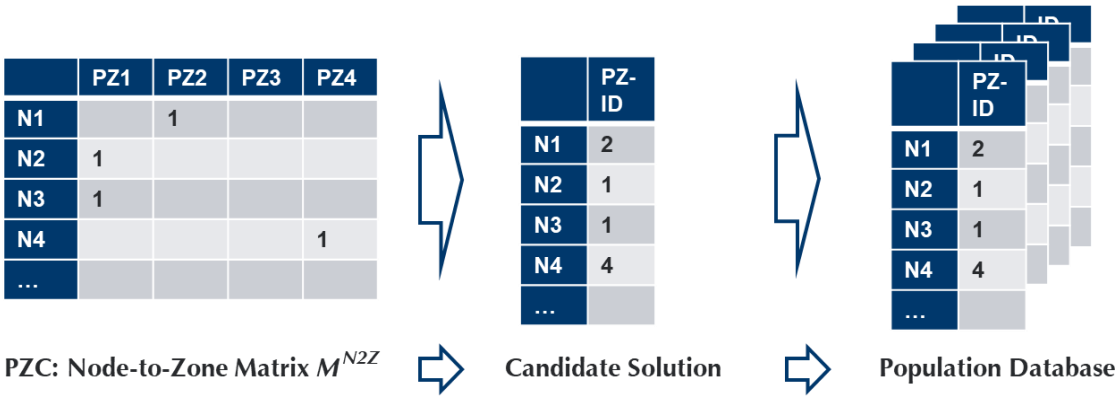

Figure 3: Transformation of node-to-zone matrix to candidate solution

For the initial population a mixture of randomly chosen PZCs and/or existing, exogenous PZCs can be chosen - the corresponding methodology of how to obtain random PZCs is described in sub-section 4.4.4. The initial population, as any other later generated candidate solution, is directly evaluated. The following sub-section discusses this process.

4.3 Evaluation

Each candidate solution is evaluated to obtain its objective value. As presented in the optimization problem of section 3, the objective value corresponds to the total SC.

However, since a candidate solution sets and fixes the node to zone assignment $M_{z,i}^{N2Z}$, the matrix $M_{z,i}^{N2Z}$ is now a parameter instead of a variable. Hence, the two levels of the presented bi-level problem can be solved sequentially. The DA-problem is solved first for each considered hour. Subsequently, costs and amounts of RD are assessed. Aside of the key indicator SC, further parameters are thereby determined that provide information for the latter applied genetic operators. Among these secondary indicators are the following:

- Adjusted SC per zone: Generation costs per zone are assessed with an adjustment for the net (export/import) position of the PZ. The net position is weighted with the average price of CWE.
- Congested lines after DA market clearing (before RD)
- Shadow prices of lines from DA problem
- Shadow prices of lines from RD problem
- Binary, sparse vector of all lines with "ones" indicating a cross-border line to evaluate equality of candidate solutions

Having introduced the concept of PZCs as candidate solutions and their evaluation (computation) methodology, the following sub-sections present the four developed genetic operators (sec. 4.1) and the selection process (sec. 4.5) indicated by the five blue boxes in Figure 2.

4.4 Genetic Operators

In total, four main operators are developed in the course of the implementation of the GA. The basic concept of commonly known operators (as "Mutation" or "Crossover") and operators that have been applied in a similar context (such as the "Split-And-Merge" operator (c.f. (Breuer, 2014)) are taken up and adapted to solve the presented bi-level problem. Especially, the "Crossover" and "Split-And-Merge" operators are reinterpreted and individually adjusted, i.e. they incorporate the introduced indicators (cf. sec. 4.3) to support the convergence towards an improved solution. In addition, the "Random" operator is newly developed to ensure the diversification of results. As the following subsections introduce, each operator puts a different emphasis on the above-introduced directions of diversification or intensification of results.

4.4.1 Mutation

This operator aims at improving local optima, thus intensification of results. Similar to the mutation operator in (Breuer, 2014), a random number (up to a pre-defined maximum number)

of border-nodes of a randomly chosen PZC receive a new PZ-ID, namely the PZ-ID of the corresponding neighboring PZ. In the latter application, for up to three PZCs a range of one to five nodes are selected and receive a new PZ-ID.

4.4.2 Crossover

The goal of this operator is, one the one hand, to create relatively new candidate solutions, and, on the other hand, to improve the selected candidate solutions. Thus, the operator aims at a combination of both diversification and intensification. The operator works as follows: A number of random candidate solutions is selected. Subsequently, the *n* zones of the first candidate solution with the least contribution to (adjusted) SC are taken and form the first zones of the new solution. The contribution of a zone is determined by its adjusted SC (c.f. section 4.3) divided by the square of the zone's number of nodes. The division ensures that larger zones with comparable costs per node are preferred over smaller zones. Thereafter, the *n* zones from the next candidate solution with the least contribution to SC are taken, provided that these zones do not - or only partly - contain nodes that already have been taken. The operator stops, when all nodes have been assigned to a zone or the maximum number of zones is reached. The repair function (c.f. sec. 4.6) handles cases where nodes have not been assigned to a zone or the maximum number of zones has not been reached.

In the later application between two and five candidate solutions are selected while the number of *n* zones, that are selected during each iteration, is set to one. Notably, only zones that are different, i.e. have different cross-border lines, are eligible for the crossover operator.

4.4.3 Split-and-Merge

The idea of the Split-and-Merge operator is to improve a candidate solution by adjusting the set of cross-border lines. This eventually enables a better congestion management by considering these lines directly in the FBMC problem. Therefore, as in (Breuer, 2014), one zone is split along a chosen line while at the same time two zones are merged. Thus, this operator focuses on both intensification and diversification of results, while the emphasis on intensification is higher.

To find a suitable line that splits a zone, the following approach is developed. One or a combination of the following criteria is randomly selected: Either a zone with high redispatch costs is chosen first and then a line of this zone is selected second or in turn, a line is selected first that determines the zone to be split. The probability for one of the two variants is 50%. The line is selected from a list of lines with (i) most overloaded lines before RD, (ii) highest shadow prices in the DA-problem or (iii) highest shadow prices in the RD-problem. With a (pre-defined) low probability – e.g. 1% in the later application - a random line is chosen.

Analogously, two zones are merged that are connected by lines that are, in the best case, neither congested before RD nor have shadow prices in either DA or RD problem.

4.4.4 Random

This operator ensures the diversification of solutions, thus prevents the algorithm to run in a local minimum. Every *n* iterations a set of random candidate solutions is created and added to the population database. Moreover, a set of random candidate solutions form the initial population database.

The operator works as follows. A particular number of nodes (equal to the number of PZs) is randomly chosen from all nodes. Each of these nodes forms the nucleus for a new zone. Subsequently, all direct neighbours to a node, if not yet belonging to another zone, are added to the zone of the node. This is repeated iteratively for each of the selected nodes until each node is assigned to a zone.

Randomly generated solutions are likely to have comparatively high objective values, especially when the algorithm has already developed a good solution over some iterations. To avoid that the random candidate solutions are immediately removed from the population database in the selection process, they get the opportunity to evolve over a limited number *n* of iterations before they compete with the other candidate solutions in the selection process. In the later application, *n* is set to 20.

4.5 Selection

In contrast to the above-described operators, the selection process does not adjust the candidate solutions. The process determines which of the new candidate solutions are taken to the next iteration, thus added to the population database and, analogously, which of the candidate solutions from the population database are replaced by new candidate solutions.

More specifically, a pre-defined number of the best solutions is taken from each, the database of existing solutions and the new solutions, while the rest is chosen from the aggregate of both new candidate solutions and population database. An exception, as described in section 4.4.4, are the randomly assessed candidate solutions. In the later application, 100 candidate solutions in each iteration form a new population. Five of them are selected of each the database and the new solutions while the remaining candidate solutions are chosen from the aggregate of both sets.

4.6 Repair Function

Comparable to the repair function in (Breuer, 2014), the developed repair function in this paper checks any violation of constraints of the node-to-zone matrix. Typical violations are nodes or

areas without a zone (i.e. without a PZ-ID) or zones consisting of two or more separate areas that are not physically connected by a transmission line. In this case, the repair function repairs the candidate solution with least invasive effort. Separate nodes and areas that have not been assigned to a zone are connected to the nearest neighboring zone. In case a zone consists of two separate areas that are not physically connected, the smaller area is connected to a neighboring zone.

Alternatively, solutions with violated constraints could be penalized with an additional term that is added to the objective function. However, for this algorithm computation time is crucial. Therefore, this repair function is directly applied before the candidate solution is evaluated.

5 Application Case and Assessment Approach

Following the methodological description, this section introduces the investigated scenarios and sensitivities and the key indicators that are applied for their assessment.

5.1 Scenarios and Sensitivities

Results are assessed for the year 2020 for all countries where currently FBMC is carried out plus Switzerland (i.e. CWE+). The grid model considers the entire geographical scope and comprises about 2300 nodes and 4400 branches and transformers. Grid expansion is considered based on (Amprion et al., 2017) while amounts of infeed from renewables are modelled based on (R2b, 2017).[10]

The nodal set-up, as explained in the literature review (cf. section 2), serves as benchmark for all investigated PZCs. Aside from the endogenous PZCs from the GA, PZCs from the HCA from (Felling and Weber, 2018) are considered for comparison. In addition, historical PZCs, i.e. the business-as-usual configuration (BAU-C) and the former common German-Austrian PZC, and expert-based PZCs from the Bidding Zone Study serve as references. The following sub-section shortly sketches the considered PZCs.

5.1.1 Nodal set-up

The SC of the nodal set-up serve as the reference value when comparing different PZCs. Costs of the other PZCs are denoted as the delta to the costs of the nodal set-up. That eases the interpretation of results and visualizes the difference to the best-case scenario.

5.1.2 Endogenous price zone configurations by a hierarchical cluster algorithm

To evaluate potential improvements of the GA in reference to existing cluster algorithms from the second stream of literature, results are compared to solutions from the HCA developed in (Felling

[10] The regarded scenario and grid model is the same that is investigated in (Voswinkel et al., 2019).

and Weber, 2018). For the detailed methodology, we refer to that paper and only briefly summarize the key functionalities here: The algorithm clusters LMPs based on a set of representative hours (possibly taken from different years) into zones. The objective function aims at the minimization of price variations within zones. Thus, the algorithm places congested lines, on which prices diverge, rather between than within zones.

5.1.3 Exogenous price zone configurations

By comparing the solutions of the GA and HCA to exogenous PZCs, the potential improvement of newly identified PZCs can be evaluated, especially in comparison to the BAU-C. Moreover, the accuracy of PZCs based on expert-guesses can be examined. Among the exogenous PZCs are the following:

Real or historical PZCs:

- GER/AT split: Business as usual with separation of German and Austrian PZ
- GER/AT common: The former BAU-C with a common German and Austrian PZ

Approximated expert guesses from the BZS[11]:

- Big Country Split 1: Split of Germany and France into a northern and southern zone each
- Big Country Split 2: Split of Germany and France into three zones each
- GER SN: The German split of "Big Country Split 1" with a common French PZ.
- GER SNW: The corresponding split of "Big Country Split 2" with a common French PZ
- Small Country Merge: Belgium and Netherlands are merged to a single PZ

5.2 Indicators

Obviously, SC are the most important key figure, since they are directly taken into account in the objective function of the GA. To evaluate these costs, the SC are broken down into RDC and MCC and compared to SC of the above-mentioned PZCs.

Aside of SC, rents and distributional effects are of high practical importance, especially given the political relevance of the topic. Therefore, equations (*23*)-(*25*) present the equations for producer, consumer and congestion rents.

In eq. (*23*) each generator is assigned its zonal DA price $p_{z,h}^{DA}$ by multiplication with the assignment matrices $M_{g,i}^{G2N} M_{z,i}^{N2Z}$. Cumulating the values of each generator yields the overall producer rent. In turn, eq. (*24*) presents the consumer rent. The value of loss load $p^{loss-load}$ is

[11] Notably, the PZCs from the BZS are approximated given the descriptions and figures in the BZS. A detailed node-to-zone assignment is not available and would not perfectly fit as different underlying grid models are used. In addition, the geographical scope in the BZS exceeds the present scope. Thus, results of these PZCs will and have to be interpreted with care.

subtracted by the zonal price at each node ($p_{z,h}^{DA} M_{z,i}^{N2Z}$) and summed over all nodes and hours. The value of $p^{loss-load}$ is set to 1000 €/MWh, however, as we only look at differences between rents of PZCs, this value cancels out. Eq. (25) finally presents the congestion rent as last relevant equation.

$$R^{prod} = \sum_{H} \sum_{G} \left(\sum_{I} \sum_{Z} (p_{z,h}^{DA} M_{g,i}^{G2N} M_{z,i}^{N2Z}) - c_{g,h} \right) g_{g,h}^{DA} \tag{23}$$

$$R^{cons} = \sum_{H} \sum_{Z} \sum_{I} (p^{loss-load} - p_{z,h}^{DA} M_{z,i}^{N2Z}) d_{i,h}^{DA} \tag{24}$$

$$R^{cong} = \sum_{Z} \sum_{H} (q_{z,h} p_{z,h}^{DA}) \tag{25}$$

Based on these equations, section 6.2.5 presents the rents for different PZCs.

6 Results

This section presents both the performance evaluation of the GA (sec. 6.1) and the assessment of its results (sec. 6.2), i.e. the resulting PZCs in comparison to other PZCs using the proposed indicators (cf. 5.2).

At first, the performance of the algorithm is investigated to illustrate its actual functionality and the convergence of its objective value to a (local) optimum. In conjunction with these results, computation times of the algorithm are presented, as they are crucial for the latter application. Furthermore, the efficiency of the genetic operators, both in interaction and separately, is examined. Second, the focus is on the determined PZCs from the GA and their assessment, i.e. the comparison to the nodal solution, to PZCs from the HCA and to exogenously given PZCs. The key indicators presented in section 5.2 serve as assessment criteria. Thereafter, conclusions are drawn regarding the solutions of the GA by comparing them to PZCs from the HCA and expert-based PZCs.

6.1 Performance Evaluation

As aforementioned, the computational performance of the algorithm is investigated at first, because it constrains, as shown in the following subsection, the number of considered hours *H* in conjunction with the number of iterations and the population size. For all of the evaluations in this section, PZCs with six zones are considered. This corresponds to the number of PZ in the BAU-C.

6.1.1 Computation time

One key advantage of the GA is that its computation can be highly parallelized. The overall computation time depends on the available system. Table 1 presents computation times for one iteration, one candidate solution and one single hour (as stated in section 3.2, the assessment of single hours is possible as no intertemporal constraints are considered). Computation of RD takes about 30 times longer than the assessment of DA markets. This is due to the difference in the number of constraints and decision variables in the two problems. While in the DA problem a limited set of lines is considered, the RD problem considers all lines, nodes and generators individually (c.f. section 3).

Table 1 Computation time

----	Computation time per single hour for one candidate solution [s]
Day-Ahead problem	Approx. 0.03 – 0.04 s
RD problem	Approx. 0.9 – 1.3 s
Total	Approx. 0.9 – 1.4 s

To get an idea of the overall computation time, the average duration for a set-up (as later used in the analysis) for 200 representative hours and 100 candidate solutions would take about 7.2 hours for only one iteration. When parallelized on six virtual machines with eight cores each, computation time for one iteration drops to about nine minutes.

However, computation time is still too high for an assessment of PZCs based on an entire year given the available computational resources. Thus, for the following analysis of the three main operators, only 10 representative hours are considered to investigate the effects of up to 1000 iterations. A sensitivity analysis for the effect of different numbers of considered hours on the objective value will be presented thereafter and conclude the performance investigation[12].

6.1.2 Effectivity of single operators

To investigate the effectivity of the operators and to get a general idea of the functionality of the algorithm, Figure 4 presents the development of the objective value (y-axis) for the ten representative hours over the number of iterations (x-axis) for the three operators “Crossover”, “Mutation” and “Split-And-Merge” as well as their combination (solid lines). We do not consider the “Random” operator, as its isolated application without the three other operators is of limited informative value.

[12] To assess the set representative hours *H*, we use k-means algorithm to cluster the residual load of the six PZ from the BAU-C into representative hours.

The dotted horizontal lines support a visual interpretation showing a corridor of the objective values between the optimal nodal solution (blue dots), the solution from the HCA[13] (yellow dots) and the BAU-C.

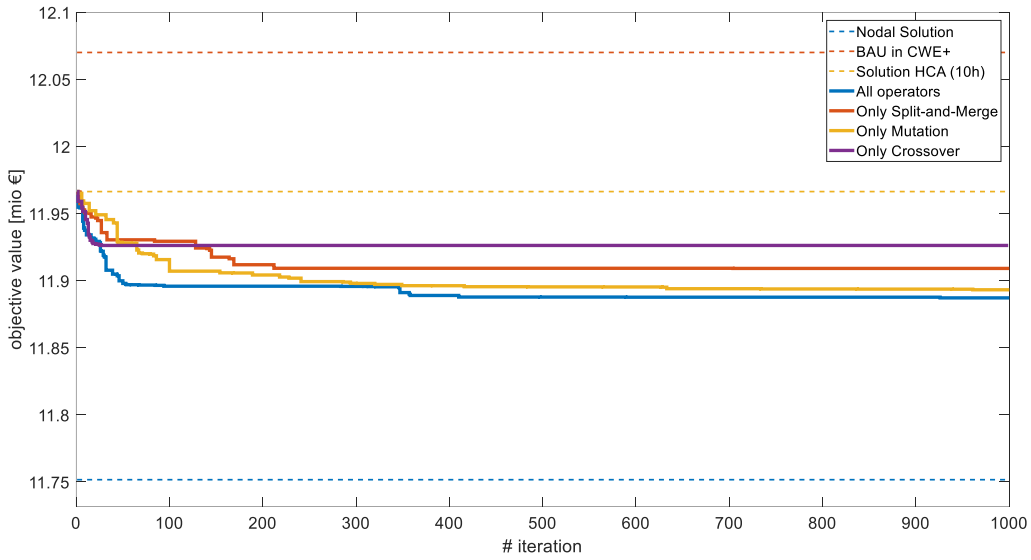

Figure 4: Development of objective value depending on number of iterations

The solid blue line indicates the development of the objective value using all three mentioned operators[14] while the other lines indicate the development when only one of the three genetic operators, "Split-and-Merge", "Crossover" and "Mutation", is applied. All four applications use identical start solutions consisting of a set of random solutions, the BAU-C and the solution from the HCA. As the start of the four lines indicates (x = 0), the PZC from the HCA has the lowest objective value, i.e. is the best solution in the initial population.

The slope of the blue line, when all fours operators are applied, is the steepest and leads to the lowest objective value in the end. Notably, the curve of the "Crossover" operator has a comparable gradient in the beginning, yet reaches a first plateau after about 30 iterations. The objective value from thereon even remains unchanged as the diversity of remaining candidate solutions decreases until all candidate solutions are the same. In the later application, this effect is avoided by mixing the operators and adding candidate solutions from the random operator. The curve of the mutation operator (yellow) drops slowly but constantly and reaches the second-best objective value after 1000 iterations. It even reaches the same objective value as the blue line around iteration 300. This course is due to its feature that only cross-border nodes are changed. Thus, changes in the PZC between iterations are not as drastic as potential changes from the other operators. In contrast, changes in the shape of PZs can be more drastic when using

[13] The HCA is also based on the LMPs of the same considered ten hours
[14] Each of the three operators receives 30% of the candidate solutions, while 10% are added by the "Random" operator.

the “Split-and-Merge” operator (orange line). Finally, all solutions reach objective values after 1000 iterations that are an improvement in comparison to the solution from the HCA and the BAU-C.

A visualization of the four resulting PZCs is given in Figure 5 - Figure 8. All Figures have similarities such as a zone encompassing large parts of France and a zone connecting Southern Germany and Austria and (varying) parts of Switzerland. Moreover, the final PZCs for the “Only Mutation” and “All operators” application are, as their objective value suggests, very alike. Regarding the PZCs from the “Only Split-and-Merge” and “Only Crossover”, there are bigger differences in Northern Germany and the BeNeLux-Countries.

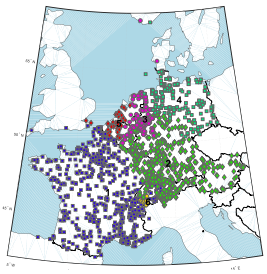

Figure 5: PZC using only Split-And-Merge

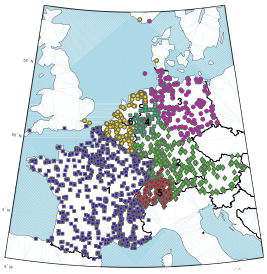

Figure 6: PZC using only Crossover

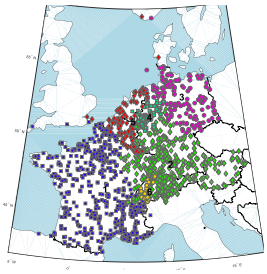

Figure 7: PZC using only mutation

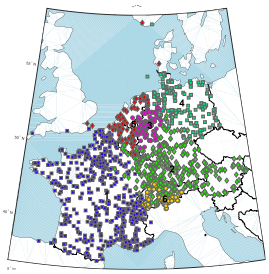

Figure 8: PZC using all operators

Notably, by definition of a GA, there is a lot of randomness involved during the application. Hence, the visualized examples only indicate a typical course of the operators.

Having introduced the basic features of the algorithm, the following section investigates the effect of considering different numbers of representative hours.

6.1.3 Evaluation of the number of representative hours

The results of section 6.1.2 are based on 10 representative hours. In this section, results for 10, 25, 100 and 200 representative hours are compared to evaluate the effect of using such a limited number of representative hours. To this end, the SC of each PZC are not only assessed for its underlying set of representative hours (“In Sample”), but also for the other sets of representative hours and the entire year (“Out of Sample”).

Starting point of the investigation are the resulting PZCs. Figure 9 – Figure 11 present the corresponding shapes. The PZC based on 10 hours remains the same as given in Figure 8.

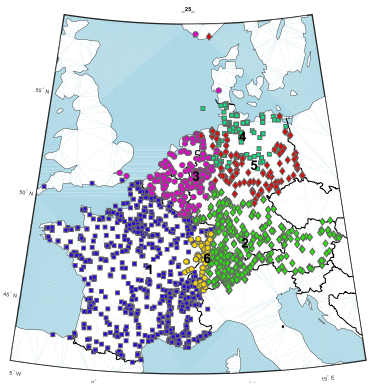

Figure 9: PZC based on 25 hours

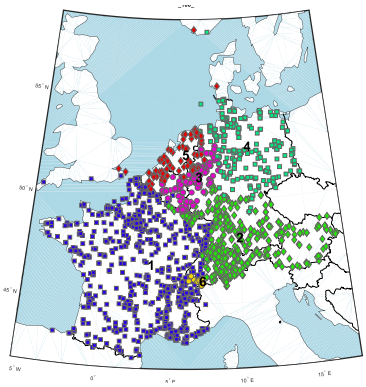

Figure 10: PZC based on 100 hours

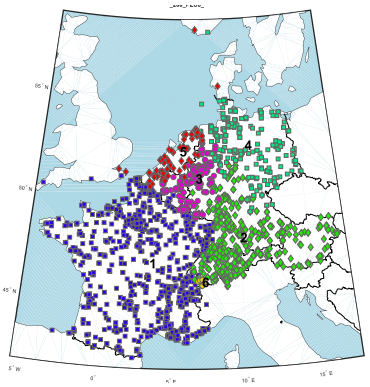

Figure 11: PZC based on 200 hours

Again, PZCs have similarities such as a joint German-Austrian PZ and a large French PZ. Main differences are found in Alsace (close to the French-German Border) and in Switzerland or in the assignment of nodes to zones in the BeNeLux area. Northern Germany is only split in more zones for the case of 25 hours.

The different shapes affect the corresponding SC as shown in Figure 12. The groups of bars indicate the results of the four different PZCs for in total five different sets of representative hours: The four sets from the GA application and an additional set that comprises the entire year (right-hand side). The presented costs are the average hourly delta to the cost from the optimal solution from the nodal set-up for the same corresponding set of hours. The absolute difference in SC is hence divided by the corresponding number of considered hours to ease comparison of results. Within each group, each bar shows the delta for the PZC based on 10, 25, 100 and 200 evaluation hours. The star in each group highlights the lowest delta to the nodal SC.

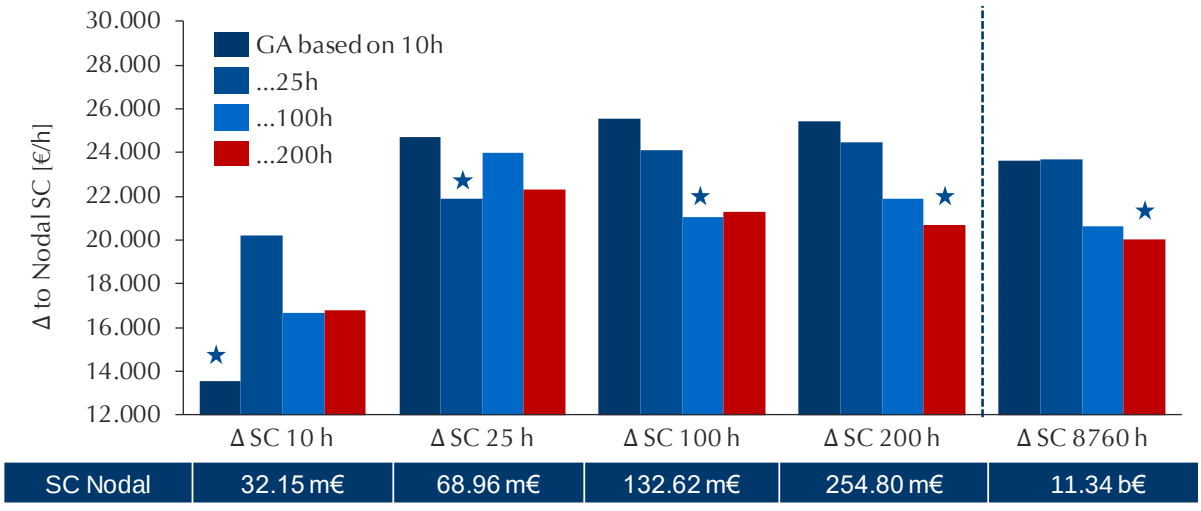

Figure 12: SC for PZCs based on different representative hours

As the stars visualizes, each PZC is the best configuration for its set of representative hours. When evaluating over the entire year, the difference in costs amounts to almost 30 m€ (i.e. around

3.7 k€/h). In total, the SC of the PZC based on 200 hours is only around 175 m€ more expensive than the nodal solution (i.e. around 20 k€/h).

The investigation of different numbers of representative hours shows that the GA and its four operators work effectively together. Moreover, the assessments indicate that a higher number of considered hours improves the SC for the entire year ("Out of Sample") and provides no evidence of local instead of global optima being selected. Differences are observed both regarding SC and shapes of PZCs. Since considering more hours improves SC for the entire year significantly, the following section now investigates PZC based on 200 hours. Moreover, the subsequent section goes into more detail regarding RDC and MCC and by extending the range of considered PZCs to further exogenously and endogenously given PZCs.[15]

6.2 Assessment of PZCs

The previous section has focused on the performance of the algorithm. Subsequently, its results, i.e. the PZCs, are examined. Starting point of the following investigations is the presented PZC based on 200 representative hours for six PZs.

The investigation is now extended in two directions.

1. The set of considered PZCs is enlarged by using the GA to determine configurations with 12 and 24 zones, i.e. the double respectively quadruple number of PZs compared to the previous PZC.
2. The set of PZCs is enlarged that the solutions from the GA are compared to. Next to the nodal solution, the BAU-C and solutions from the HCA, we now also investigate exogenously given, expert-based PZCs from the BZS.

The next sub-section commences by introducing the shape of the PZC for 12 and 24 zones before their results are compared to (a) the resulting PZCs from the HCA and (b) exogenously given PZCs. All investigations assess costs for an entire year.

6.2.1 Results from the Genetic Algorithm

Figure 13 and Figure 14 present the PZC for 12 and 24 PZ. The PZC for six PZs remains unchanged (cf. Figure 11).

[15] The maximum number of iterations remains at 1000. However, usually the best configuration, comparable to the results presented in Figure 4 , is identified after 300-400 iterations.

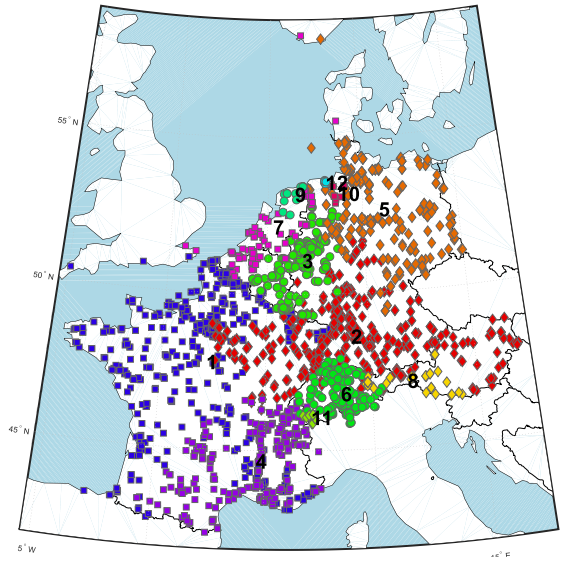

Figure 13: Shape of PZC with 12 PZ from GA (GA 12-ImpC)

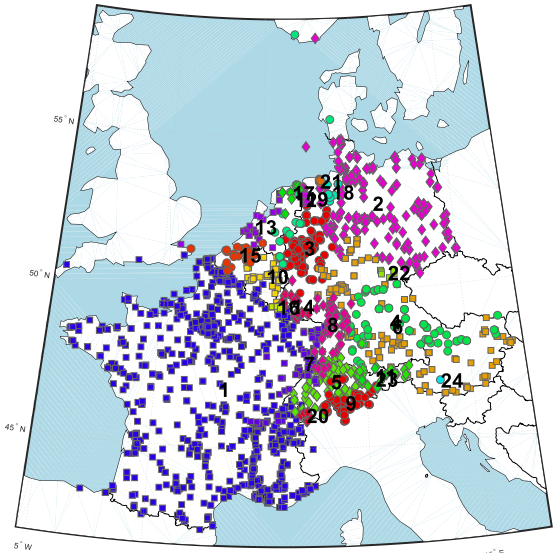

Figure 14: Shape of PZC with 24 zones from GA (GA 24-ImpC)

In comparison to the improved configuration with 6 zones (short: 6-**ImpC**) now parts from Austria separate from Southern Germany and the French PZ splits into more than one PZ. Thereby the borders of PZs of the 6-ImpC, 12-ImpC and 24-ImpC are independent from each other in contrast to solutions from the HCA as will be shown in the following subsection. Due the hierarchical (or greedy) structure of the HCA, PZs from a configuration with a smaller number of zones are always subsets from PZCs with more zones. This is not the case for the GA.

Similar to sections 6.1.2 and 6.1.3, the different shapes (and numbers) of PZs imply variations in SC. Figure 15 presents the costs components of RDC, MCC and SC. For now, the focus is on the bars of the "Genetic Algorithm" group on the left. Again, costs are denoted as the delta to the nodal SC for an entire year. For each configuration, three bars indicate the MCC (dark blue), the RDC (light blue) and the SC (red) as difference to the optimal nodal solution. As the DA market problem is less restrictive than the nodal problem, MCC are always lower compared to the nodal solution. However, these savings come at costs in terms of RDC. These are non-existent in the nodal set-up (at least as it is modelled here). Together, MCC and RDC add up to the SC that are visualized in the third, red column.

As expected, when increasing the number of PZs, costs decrease. By doubling or quadrupling the number of PZs, the delta to the nodal system decreases by more than 50% to 86 m€. The DA problem gets more restrictive, thus MCC increase (i.e. the delta to nodal decreases) while RDC decrease. Since the decrease in RDC is stronger, the overall SC decrease as well.

Having introduced the three PZCs from the GA, their results are now compared to the results from the HCA in the following subsection.

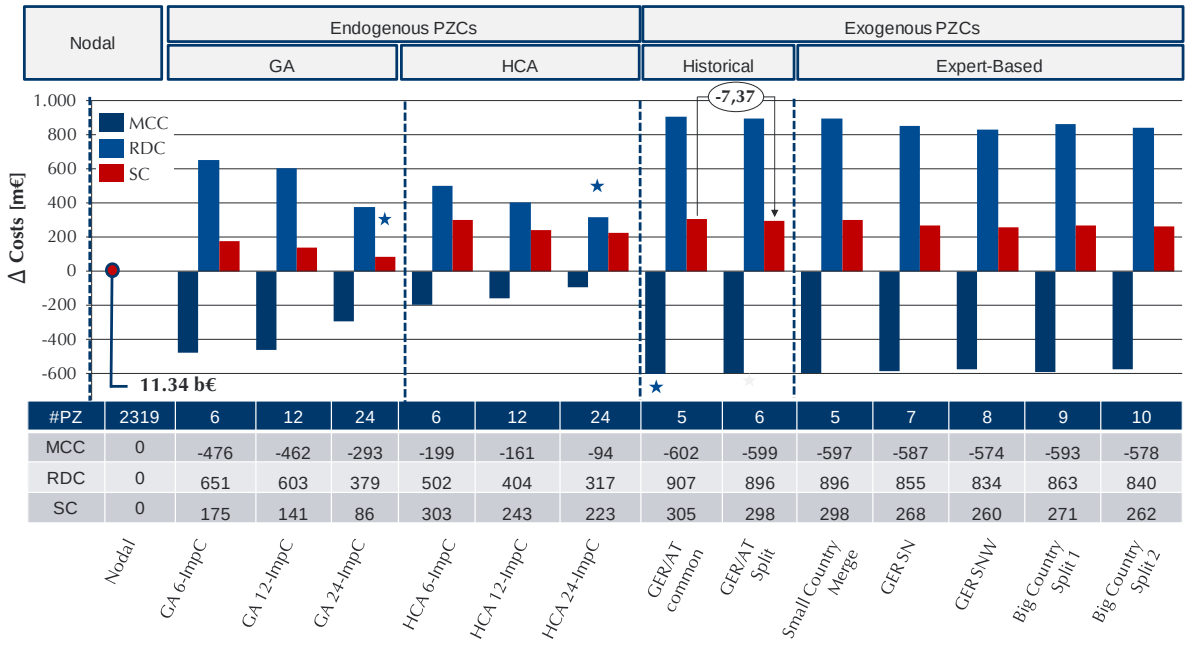

#PZ	2319	6	12	24	6	12	24	5	6	5	7	8	9	10
MCC	0	-476	-462	-293	-199	-161	-94	-602	-599	-597	-587	-574	-593	-578
RDC	0	651	603	379	502	404	317	907	896	896	855	834	863	840
SC	0	175	141	86	303	243	223	305	298	298	268	260	271	262

Nodal, GA 6-ImpC, GA 12-ImpC, GA 24-ImpC, HCA 6-ImpC, HCA 12-ImpC, HCA 24-ImpC, GER/AT common, GER/AT Split, Small Country Merge, GER SN, GER SNW, Big Country Split 1, Big Country Split 2

Figure 15: MCC, RDC and SC for different PZCs

6.2.2 Comparison to other endogenous PZCs

Again, we look at the shape of PZCs before we assess their corresponding costs. Figure 16 to Figure 18 present the solution from the HCA based on the same 200 hours.

As mentioned in section 6.2.1, the PZs from the HCA 24-ImpC and the PZs from the HCA 12-ImpC are subsets of the HCA 6-ImpC. For example, zones #8, #9, #10 and #11 in the HCA 12-ImpC form together PZ #5 in the HCA 6-ImpC. Apart of that, PZs themselves differ a lot when comparing the shape of PZs from HCA to the GA.

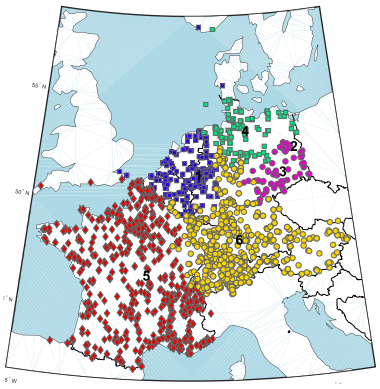

Figure 16: Improved PZC for 6 PZ from HCA (HCA 6-ImpC)

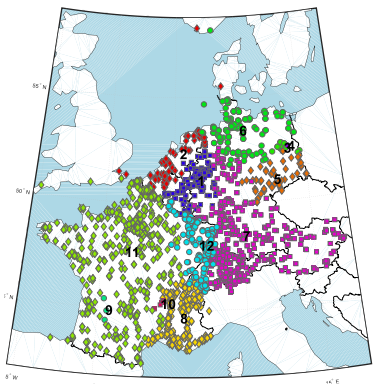

Figure 17: Improved PZC for 12 PZ from HCA (HCA 12-ImpC)

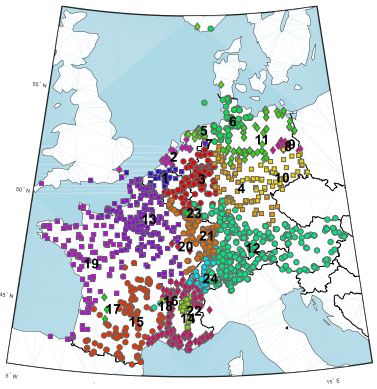

Figure 18: Improved PZC for 24 PZ from HCA (HCA 24-ImpC)

In terms of SC, neither of the PZCs from the HCA achieves as good results as the GA solutions. The costs are denoted in the group "Hierarchical Cluster Algorithm" in Figure 15 next to the previously presented results from the GA. In fact, when comparing the results of the GA and HCA

with the same number of zones, cost differences arise to 127 m€ for the 6-ImpC, around 100 m€ for the 12- and 137 m€ for the 24-ImpC, respectively.

On the other hand, the following point is worth noticing: All solutions from the HCA achieve best results in terms of RDC. To push further - and without going into too much detail regarding the exogenous PZCs - the RDC are even the lowest throughout all considered PZCs. Thus, the comparably high SC result from high MCC. This effect explains as follows: The algorithm aims at finding zones with similar prices, thus placing congested lines rather between than within PZs. This goal is achieved, as the low RDC suggest. However, these PZ borders lead to unnecessary high MCC, probably as the DA-problem gets too restrictive. A similar effect is observed and described in (Felling et al., 2019). Thus, the algorithm achieves its goal of identifying congestions and placing these lines between zones, however, as market costs are not in the scope of the algorithm, this eventually leads to high overall costs. Hence, the application of this kind of algorithms that are based on approximate criterions such as LMPs is questionable when determining PZCs.

6.2.3 Comparison to exogenously given PZCs

The previous two sub-sections compared the results from the endogenously assessed PZCs. The following section now puts focus on exogenous PZCs. These comprise the BAU-C and the former BAU-C with a common German-Austrian PZ. Moreover, results are assessed for the expert-based PZCs from the BZS that have been introduced in section 5.1.3.

As the PZCs for the BAU cases are straightforward, Figure 19 and Figure 20 present the expert-based PZCs for the so-called "Big Country Split 1" and "2".

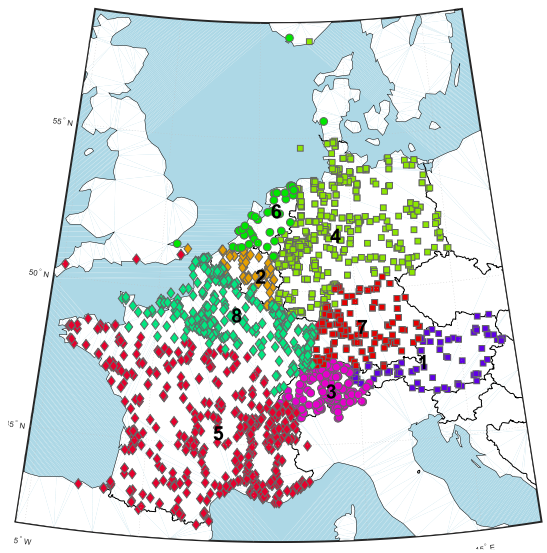

Figure 19: Big Country Split 1

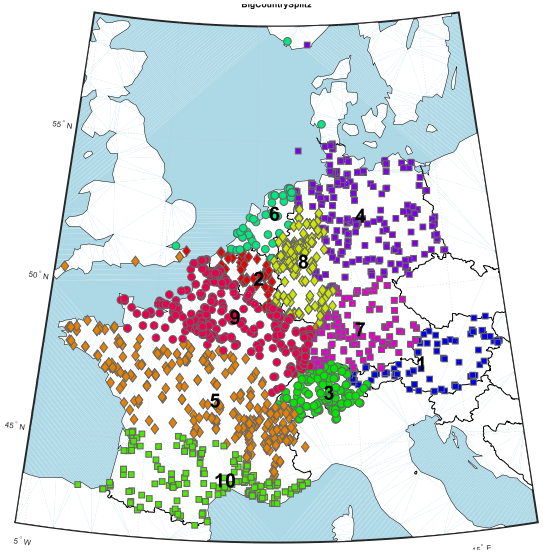

Figure 20: Big Country Split 2

A split of the French and German PZs into two respectively three zones each leads to savings of around 27 m€ for the "Big Country Split 1" and 35 m€ for the "Big Country Split 2" in reference

to the BAU-C. Notably, the savings for the same German splits with a united French PZ even achieve slightly better results including slightly lower RDC (around 2 m€). (However, this does not hold for the absolute RD amounts as the following sub-section reveals.) The split of the German-Austrian PZ saves 7 m€ in SC while RDC drop by about 11 m€. These amounts appear not that significant. Reasons for the rather low savings could be the analyzed scenario 2020 with an optimistic grid expansion but also the inefficiency of the proposed exogenous splits.

When comparing these results to the PZCs from the GA, the latter achieves higher savings. Just by reshaping the borders of the BAU-C and, thus, maintaining six zones, SC drop by 123 m€. When increasing the number of PZs, costs drop even further to 157 m€ for the 12-ImpC and 212 m€ for the 24-ImpC, respectively. In relation the overall SC of the BAU-C (11.65 b€) this corresponds to savings of 1.8%.

Notably, SC from the 6-ImpC from the HCA are between the two BAU-C. Nevertheless, as anticipated in section 6.2.2, RDC drop by 400 m€ and are the lowest for any PZC with 6 zones. As aforementioned, the RDC for the 24-ImpC are the lowest throughout all PZCs. In the following section, the RD amounts corresponding to the presented costs are shown.

6.2.4 Impact on redispatch amounts

While Figure 15 showed the RDC, Figure 21 presents the corresponding RD amounts (in positive direction) in TWh for each PZC. To ease interpretation of results, PZCs are ordered in the same way. The order of RDC does not necessarily corresponds to the order of quantities. The 24-ImpC from the HCA has least RDC, yet the 24-ImpC from the GA achieves lowest quantities, as the blue star indicates. This also holds for the 12-ImpC from the HCA and GA. RD amounts of the Big Country Splits are lower than the amounts of the corresponding German splits while it is the other way around for RDC. However, differences are rather small.

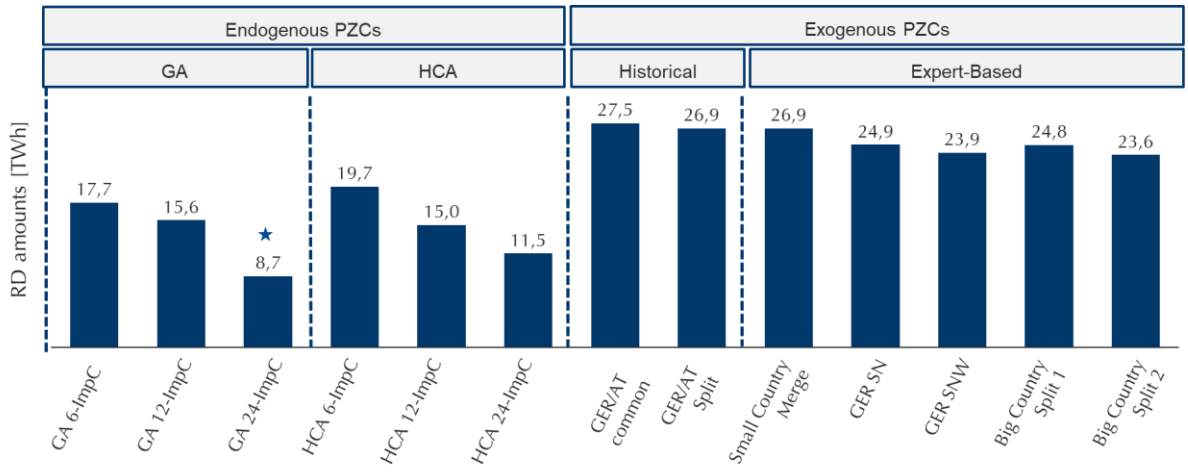

Figure 21: Redispatch amounts for all PZCs [in positive direction in TWh]

In total, RD amounts drop from 26,9 TWh in BAU-C by reshaping the borders to the 6-ImpC (GA) to 17,7 TWh. When adding more zones, RD amounts drop further to 8.7 TWh. That is less than one third of the quantities of the BAU-C.

6.2.5 Impact on rents

Figure 22 presents the producer, consumer and congestion rents for selected PZCs for CWE. Figure 22 only shows the rents for the two German Splits from the exogenous PZCs, as differences are rather small in contrast to the endogenous PZCs. In contrast to the previous sections, Figure 22 indicates the rents of the market clearing stage in reference to the BAU-C. The delta to the nodal system is denoted at the bottom of the figure. Under the chosen assumption of cost-based redispatch, no rents arise at the redispatch stage. Yet, obviously the redispatch costs have to be borne by some of the stakeholders – according to the current rules in Germany these costs are passed through by the grid operators to the consumers.

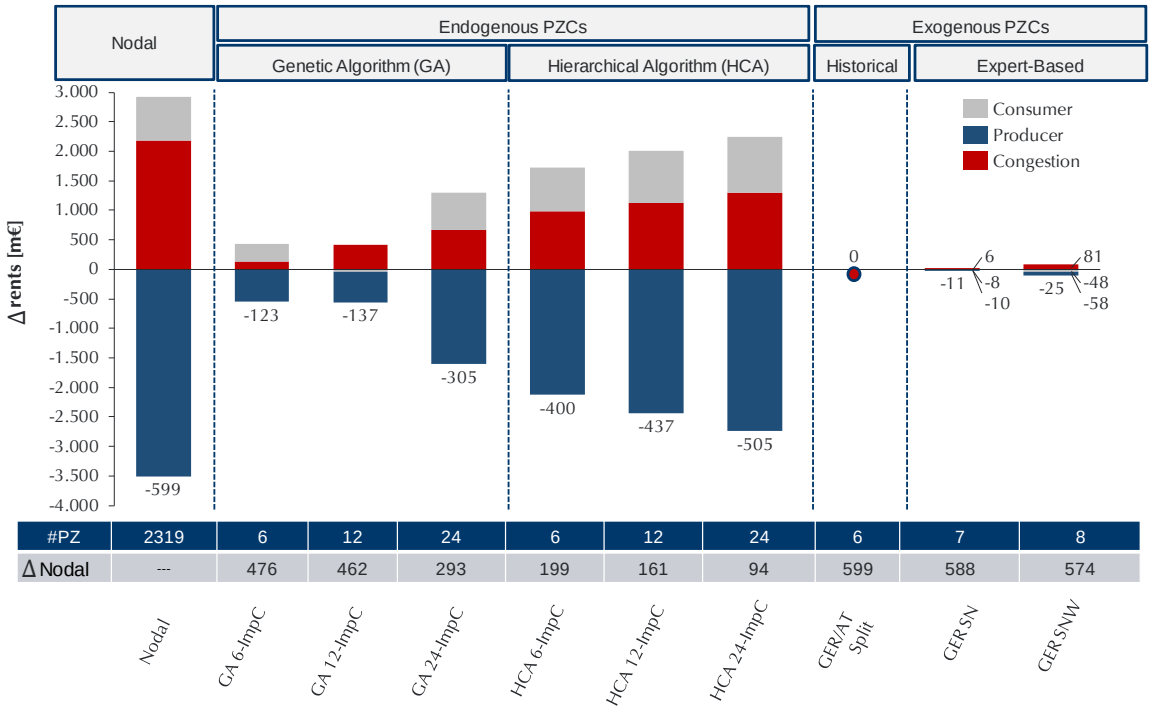

Figure 22: Rents for selected PZCs for entire CWE.

Overall, the decreases of producer rents are striking, especially for the nodal system and the configurations from the HCA. The higher the number of zones, the better local scarcity and congestions are reflected in market prices. This causes especially **producer rents** of RES to decrease massively. Figure 23 visualizes producer rents for Germany in reference to the BAU-C. Rents from wind generation, both from On- and Offshore, decrease significantly. In the nodal system, producer rents drop by almost 3 b€. In turn, producer rents from conventional power plants increase slightly. Effects for the exogenous PZCs are rather small.

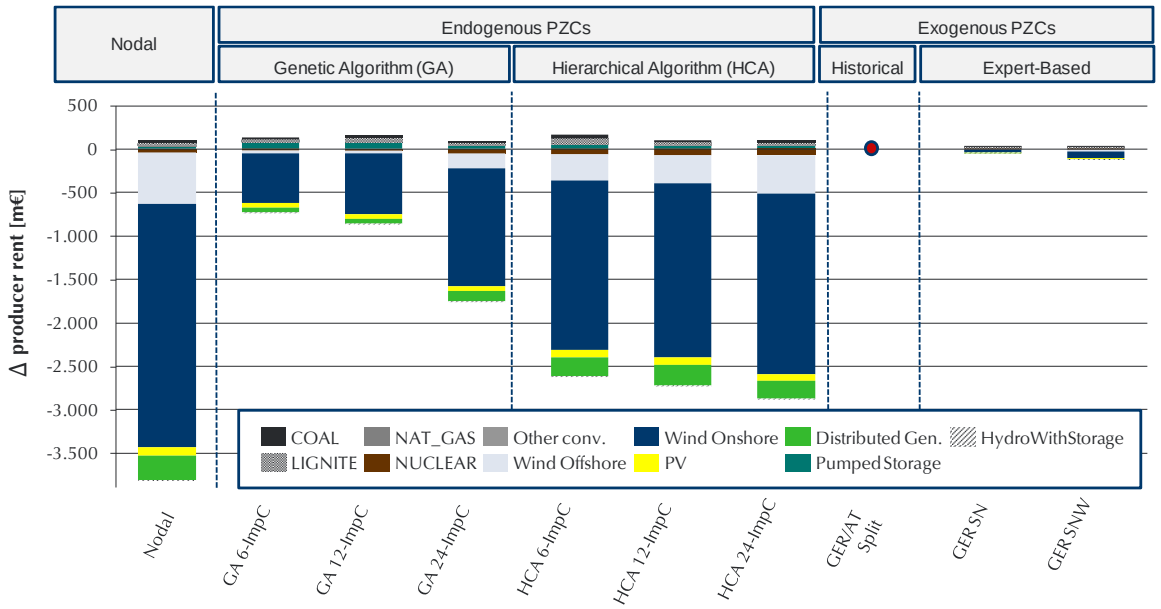

Figure 23: Producer rents for Germany

In parallel to decreasing producer rents, **consumer rents** increase in almost all cases. Table 2 presents consumer rents for CWE by country, again, in reference to the BAU-C. In the 24-ImpC (GA), consumers in Germany benefit from decreasing prices with a total of around 600 m€. In the nodal solution, the consumer rent is even higher (>1 b€). Notably, the 12-ImpC (GA) is the only case of the endogenous PZCs where total consumer rent is negative. This is due to the shape of PZs. In the 12-ImpC (GA), PZ #2 stretches from France overs southern Germany towards Austria (cf. Figure 13). Hence, prices increase, especially for the French region that usually profits from local low-cost nuclear power stations. This causes consumer rent in France to drop significantly (-357 m€) in comparison to the 6-ImpC (-69 m€) and 24-ImpC (-188 m€) from the GA.

Finally, **congestions rents**, as expected, rise when switching to a nodal pricing regime or endogenous zones with more price zones.

Table 2: Consumer rent for CWE on PZ level (in m€)

Country (PZ) Nodal	6-ImpC (GA)	12-ImpC (GA)	24-ImpC (GA)	6-ImpC (HCA)	12-ImpC (HCA)	24-ImpC (HCA)	GER SN	GER SNW
AT -5,3	-20,9	-16,3	-8,2	-13,4	-19,7	-13,4	-7,3	-8,9
BE -54,1	43,7	10,0	47,3	15,1	28,5	-4,8	-2,7	11,0
CH 40,4	75,7	63,8	73,4	45,5	34,6	36,6	3,8	-1,7
DE 1029,8	242,0	244,6	607,3	909,1	1006,0	1004,7	3,7	-2,7
FR -315,9	-69,2	-357,5	-188,7	-238,0	-217,4	-224,5	5,1	-15,9
BE 37,4	22,2	16,3	104,6	36,6	44,6	143,4	-10,3	-29,2
Total 732,2	293,5	-39,1	635,6	755,0	876,5	942,0	-7,6	-47,6

7 Conclusion and Outlook

The paper at hand introduces a novel approach to identify improved PZCs, namely a bi-level optimization problem. For its solution, a problem-specific and tailored genetic algorithm is developed. The algorithm is applied to the entire system of CWE+. Results show that the new algorithm achieves the best results in terms of overall SC in comparison to all other investigated PZCs. In reference to the BAU-C, costs decrease by 123 m€, 157 m€ and 178 m€ for 6, 12, and 24 zones, respectively. Just by reshaping the borders of the BAU-C and maintaining six PZs significant savings in both RDC and SC are realized. Moreover, the presented approach is the first that combines all three introduced streams in the extant literature.

In reference to the hierarchical algorithm of (Felling and Weber, 2018), results show that minimizing RD does not necessarily lead to minimal SC. While RDC of the HCA are lowest in comparison to the solutions of the GA, their overall SC are significantly higher. This underlines

the importance of considering both MCC and RDC for an evaluation of PZCs and, correspondingly, including both costs in the objective function of an algorithm. It also substantiates the findings regarding the HCA of (Felling et al., 2019) that peculiarities of FBMC should be considered when determining new PZCs.

A comparable HCA that does neither consider overall SC nor FBMC in its objective function has been proposed in the Bidding-Zone Study (ENTSO-E, 2018) to delimitate new PZCs for CWE and further parts of Europe.[16] Additionally, the proposed exogenous splits from the BZS investigated in this paper appear to be inefficient, at least for the considered scenario and the used modelling approach. Accordingly, policy-makers should carefully select the methods for identifying improved PZCs. The same applies for the evaluation and comprehensive analysis of their results.

The distribution of rents shows how producer rents decrease significantly, especially in Germany, when introducing improved PZCs with a higher number of zones. In particular, RES infeed suffers from self-cannibalization effects. In turn, consumer rents over all countries increase with the introduction of endogenous PZCs. An exception constitutes the case of the 12-ImpC PZC from the GA. Therein consumer rents decrease in reference to BAU-C, because of a large southern zone that stretches from mid-France up to Austria. This underlines the sensitivity of PZCs on results: Even if the same methodology is applied, results with different numbers of zones can differ significantly. Impacts of exogenous splits on rents are, in contrast to the endogenous PZCs, rather negligible.

In terms of functionality and performance, results show that the GA and its four operators work effectively together. The numerical experiments with different numbers of representative hours indicate that a higher number of considered hours improves the SC for the entire year ("Out of Sample") and provides no evidence of local instead of global optima being selected. Given limited computation power, the maximum of considered hours in the analysis remained 200.

When considering the presented results, some aspects should be kept in mind. In this study, only one scenario with PZCs based on a maximum of 200h have been investigated. As the sensitivity study in section 6.1.3 and results in (Leisen et al., 2019; Felling and Weber, 2018) suggest, PZCs are sensitive and most probably differ when either more representative hours or scenarios are considered. Other important factors that drive results are the mark-up factor γ for RDC and the simplified market- and redispatch model that do not consider intertemporal constraints.

Thus, future work could focus on applying the algorithm on a high performance cluster to increase both the number of iterations and considered representative hours. Another

[16] The PZCs from the therein-applied HCA have been adjusted in a post-processing and have neither been assessed with a market nor a redispatch model.

improvement would be the modelling of intertemporal constraints to increase validity of results. Sensitivity studies could investigate the effect of adjusting FBMC parameters, i.e. consideration of internal branches or different FRMs on the shape of PZs.

References

ACER, 2018. Public Consultation on the amendments of the proposal for common capacity calculation methodology for the Core region (PC_2018_E_06). URL https://surveys.acer.europa.eu/eusurvey/runner/CORE_CCM_2018 (visited on 22.07.2019)

Amprion, 50Tennet, TransnetBW, Tennet, 2017. Netzentwicklungsplan 2030, Version 2017, Zweiter Entwurf der Übertragungsnetzbetreiber. URL https://www.netzentwicklungsplan.de/de/netzentwicklungsplaene/netzentwicklungsplaene-2030-2017 (visited on 22.07.2019)

Amprion, APX, Belpex, Creos, Elia, Spot, E., Rte, Tennet, TransnetBW, 2014. Documentation of the CWE FB MC solution. URL https://www.acm.nl/sites/default/files/old_publication/bijlagen/13001_140530-cwe-fb-mc-formal-approval-request.pdf (visited on 22.02.2019)

Bergh, K. Van Den, Wijsen, C., Delarue, E., William, D., Bergh, K. Van Den, Wijsen, C., Delarue, E., William, D., 2016. The impact of bidding zone configurations on electricity market outcomes, in: ENERGYCON 2016. Leuven. https://doi.org/10.1109/ENERGYCON.2016.7514031

Biggar, Darryl R.; Hesamzadeh, M.R., 2014. The economics of electricity markets. John Wiley & Sons Ltd. https://doi.org/10.1002/9781118775745

Bjørndal, M., Bjørndal, E., 2017. Pricing and congestion management in coupled European wholesale markets, in: Energy Lab / ENE, Kristian Gerhard Jebsen Centre, Presentation from September 13, 2017.

Bjørndal, M., Jörnsten, K., 2001. Zonal pricing in a deregulated electricity market. Energy Journal 22, 51–73. https://doi.org/10.5547/ISSN0195-6574-EJ-Vol22-No1-3

Bjørndal, M., Jörnsten, K., 2007. Benefits from coordinating congestion management-The Nordic power market. Energy Policy 35, 1978–1991. https://doi.org/10.1016/j.enpol.2006.06.014

Breuer, C., 2014. Optimale Marktgebietszuschnitte und ihre Bewertung im europäischen

Stromhandel. Aachener Beiträge zur Energieversorgung (Dissertation), Aachen.

Breuer, C., Moser, A., 2014. Optimized bidding area delimitations and their impact on electricity markets and congestion management, in: International Conference on the European Energy Market, EEM. https://doi.org/10.1109/EEM.2014.6861218

Breuer, C., Seeger, N., Moser, A., 2013. Determination of alternative bidding areas based on a full nodal pricing approach, in: IEEE Power and Energy Society General Meeting. https://doi.org/10.1109/PESMG.2013.6672466

Bundesnetzagentur, 2019. Quartalsbericht zu Netz- und Systemsicherheitsmaßnahmen. URL https://www.bundesnetzagentur.de/SharedDocs/Downloads/DE/Allgemeines/Bundesnetzagentur/Publikationen/Berichte/2019/Quartalsbericht_Q2Q3_2018.pdf?__blob=publicationFile&v=2 (visited on 22.07.2019)

Bundesverband der Energie- und Wasserwirtschaft e.V. (BDEW), 2018. Redispatch in Deutschland. Berlin. URL https://www.bdew.de/media/documents/Awh_20190326_Bericht-Redispatch_Maerz-2019.pdf (visited on 22.07.2019)

Burstedde, B., 2012. From nodal to zonal pricing: A bottom-up approach to the second-best, in: 9th International Conference on the European Energy Market, EEM 12. pp. 1–8. https://doi.org/10.1109/EEM.2012.6254665

Consentec, Neon, 2018. Nodale und zonale Strompreissysteme im Vergleich - Bericht für das Bundesministerium für Wirtschaft und Energie. URL https://www.bmwi.de/Redaktion/DE/Publikationen/Studien/nodale-und-zonale-strompreissysteme-im-vergleich.pdf?__blob=publicationFile&v=4 (visited on 22.07.2019)

Dierstein, C., 2017. Impact of Generation Shift Key determination on flow based market coupling, in: International Conference on the European Energy Market, EEM. https://doi.org/10.1109/EEM.2017.7981901

Duthaler, C.L., Finger, M., Püttgen, H.B., 2012. A Network- and Performance-based Zonal Configuration Algorithm for Electricity Systems. Lausanne, EPFL (Dissertation),

Lausanne. https://doi.org/10.5075/epfl-thesis-5387

Egerer, J., Weibezahn, J., Hermann, H., 2016. Two Price Zones for the German Electricity Market – Market Implications and Distributional Effects. Energy Economics 59, 365–381. https://doi.org/10.1016/j.eneco.2016.08.002

Ehrenmann, A., Smeers, Y., 2005. Inefficiencies in European congestion management proposals. Utilities Policy 13, 135–152. https://doi.org/10.1016/j.jup.2004.12.007

ENTSO-E, 2018. First Edition of the Bidding Zone Review - Final Report. URL https://consultations.entsoe.eu/markets/first-edition-bidding-zone-review/supporting_documents/Final report for public consultation_090218.pdf (visited on 22.07.2019)

Felling, T., Felten, B., Osinski, P., Weber, C., 2019. Flow-Based Market Coupling Revised - Part II : Improved Price Zones in Central Western Europe (No. 07 /2019), HEMF Working Paper.

Felling, T., Weber, C., 2018. Consistent and robust delimitation of price zones under uncertainty with an application to Central Western Europe. Energy Economics 75, 583–601. https://doi.org/10.1016/j.eneco.2018.09.012

Felten, B., Felling, T., Osinski, P., Weber, C., 2019. Flow-Based Market Coupling Revised - Part I : Assessing small- and large-scale systems (No. 06 / 2019), HEMF Working Paper.

Finck, R., Ardone, A., Fichtner, W., 2018. Impact of flow-based market coupling on generator dispatch in CEE region. International Conference on the European Energy Market, EEM 2018-June, 1–5. https://doi.org/10.1109/EEM.2018.8469927

Goldberg, D.E., Holland, J.H., 1989. Genetic Algorithms and Machine Learning. Machine Learning 3, 95–99. https://doi.org/10.1023/A:1022602019183

Grimm, V., Kleinert, T., Liers, F., Schmidt, M., Zöttl, G., 2017. Optimal price zones of electricity markets: a mixed-integer multilevel model and global solution approaches. Optimization Methods and Software 34, 1–31. https://doi.org/10.1080/10556788.2017.1401069

Hogan, W., 1992. Contract networks for electricity power transmission. Journal of Regulatory Economics 242, 211–242.

Holland, J.H., 1975. Adaptation in Natural and Artificial Systems. Univ. of Michigan Press, Ann Arbor, Michigan.

Imran, M., Bialek, J.W., 2008. Effectiveness of zonal congestion management in the European electricity market. 2008 IEEE 2nd International Power and Energy Conference 16–20. https://doi.org/10.1109/PECON.2008.4762432

Kang, C.Q., Chen, Q.X., Lin, W.M., Hong, Y.R., Xia, Q., Chen, Z.X., Wu, Y., Xin, J.B., 2013. Zonal marginal pricing approach based on sequential network partition and congestion contribution identification. International Journal of Electrical Power and Energy Systems 51, 321–328. https://doi.org/10.1016/j.ijepes.2013.02.033

Klos, M., Wawrzyniak, K., Jakubek, M., Orynczak, G., 2014. The scheme of a novel methodology for zonal division based on power transfer distribution factors, in: IECON 2014 - 40th Annual Conference of the IEEE Industrial Electronics Society. pp. 3598–3604. https://doi.org/10.1109/IECON.2014.7049033

Leisen, R., Felling, T., Podewski, C., Weber, C., 2019. Evaluation of Risks for Electricity Generation Companies through Reconfiguration of Bidding Zones in Extended Central Western Europe. The Energy Journal 40. https://doi.org/10.5547/01956574.40.si1.cdei

Marien, A., Luickx, P., Tirez, A., Woitrin, D., 2013. Importance of design parameters on flowbased market coupling implementation. International Conference on the European Energy Market, EEM. https://doi.org/10.1109/EEM.2013.6607298

Marjanovic, I., Vom Stein, D., Van Bracht, N., Moser, A., 2018. Impact of an enlargement of the flow based region in continental Europe, in: International Conference on the European Energy Market, EEM. IEEE, pp. 1–5. https://doi.org/10.1109/EEM.2018.8470008

Mitchell, M., 1998. An Introduction to Genetic Algorithms. A Bradford Book The MIT Press Cambridge, Cambridge, Massachusetts and London, England. https://doi.org/10.1016/S0898-1221(96)90227-8

R2b, 2017. Mittelfristprognose zur deutschlandweiten Stromerzeugung aus EEG-geförderten Kraftwerken für die Kalenderjahre 2018 bis 2022. Köln. URL https://www.netztransparenz.de/portals/1/Content/EEG-Umlage/EEG-Umlage 2018/20171011_Abschlussbericht_EE_r2b.pdf (visited on 22.07.2019)

Sarfati, M., Hesamzadeh, M.R., Canon, A., 2015. Five Indicators for Assessing Bidding Area Configurations in Zonally-Priced Power Markets, in: 2015 IEEE Power & Energy Society General Meeting. Denver, CO, pp. 1–5. https://doi.org/10.1109/PESGM.2015.7286517

Schavemaker, P., Croes, A., Druet, C., Otmani, R., Bourmaud, J., Zimmermann, U., Wolpert, J., Rexer, F., Weis, O., Druet, C., Tennet, RTE, EON, EnbW, RWE, ELIA, 2008. Flow-based allocation in the central western European region. Cigré Session C5-307.

Schweppe, F.C., Caraminis, M.C., Tabors, R.D., Bohn, R.E., 1988. Spot pricing of electricity. Springer US. https://doi.org/10.1007/978-1-4613-1683-1

Srinivas, M., Patnaik, L.M., 1994. Genetic Algorithms: A Survey. Computer 27.6, 17–26.

Tovey, C.A., 2018. Nature-Inspired Heuristics: Overview and Critique, in: Recent Advances in Optimization and Modeling of Contemporary Problems. INORMS Conference TutORial, Phoenix, AZ, pp. 158–192. https://doi.org/10.1287/educ.2018.0187

Trepper, K., Bucksteeg, M., Weber, C., 2015. Market splitting in Germany - New evidence from a three-stage numerical model of Europe. Energy Policy 87, 199–215. https://doi.org/10.1016/j.enpol.2015.08.016

Van den Bergh, K., Boury, J., Delarue, E., 2016. The Flow-Based Market Coupling in Central Western Europe: Concepts and definitions. Electricity Journal 29, 24–29. https://doi.org/10.1016/j.tej.2015.12.004

Voswinkel, S., Felten, B., Felling, T., Weber, C., 2019. Flow-Based Market Coupling – What drives welfare in Europe's electricity market design? (No. 8 / 2019), HEMF Working Paper.

Wawrzyniak, K., Orynczak, G., Klos, M., Goska, A., Jakubek, M., 2013. Division of the energy market into zones in variable weather conditions using Locational Marginal Prices. IECON Proceedings (Industrial Electronics Conference) 2027–2032. https://doi.org/10.1109/IECON.2013.6699443

Wyrwoll, L., Kollenda, K., Muller, C., Schnettler, A., 2018. Impact of Flow-Based Market Coupling Parameters on European Electricity Markets. Proceedings - 2018 53rd International Universities Power Engineering Conference, UPEC 2018 1–6. https://doi.org/10.1109/UPEC.2018.8541904

Correspondence

Tim Felling, M.Sc.

Research Associate

House of Energy Markets and Finance

University of Duisburg-Essen, Germany

Universitätsstr. 12, 45117

Tel. +49 201 183-

Fax +49 201 183-2703

E-Mail tim.felling@wiwi.uni-due.de

House of Energy Markets and Finance

University of Duisburg-Essen, Germany

Universitätsstr. 12, 45117

Fax +49 201 183-2703

E-Mail web.hemf@wiwi.uni-due.de

Web www.hemf.net